Kinetic and thermodynamic evaluation of pyrolysis of jeans waste via coats-redfern method

Rumaisa Tariq*, Abrar Inayat, Muhammad Shahbaz***, Hassan Zeb****,†, Chaouki Ghenai**,
Tareq Al-Ansari***, and Jaehoon Kim*****,******,*******,†**

*School of Engineering, Monash University Malaysia, 47500 Bandar Sunway, Malaysia
**Department of Sustainable and Renewable Energy Engineering, University of Sharjah, 27272, Sharjah, United Arab Emirates
***Division of Sustainable Development, College of Science and Engineering, Hamad Bin Khalifa University (HBKU),
Qatar Foundation, 5825 Doha, Qatar
****Institute of Energy and Environmental Engineering, University of the Punjab, Q&A Campus, Lahore, Pakistan
*****SKKU Advanced Institute of Nanotechnology (SAINT), Sungkyunkwan University,
2066 Seobu-ro, Jangan-gu, Suwon, Gyeong Gi-do 16419, Korea
******School of Mechanical Engineering, Sungkyunkwan University,
2066 Seobu-ro, Jangan-gu, Suwon, Gyeong Gi-do 16419, Korea
*******School of Chemical Engineering, Sungkyunkwan University,
2066 Seobu-ro, Jangan-gu, Suwon, Gyeong Gi-do 16419, Korea

Abstract−Used textiles, such as jeans wastes, exhibit a high potential for generating renewable and sustainable energy. However, limited research has been devoted toward investigating the kinetic and thermodynamic parameters of textile wastes during pyrolysis and applying these wastes as feedstock for fuels such as biogas. Therefore, this study investigated the kinetic and thermodynamic aspects of the thermal decomposition of jeans waste to evaluate its potential for sustainable energy production. Jeans waste was heat treated at 50-850 $^{\circ}$C under different heating rates of 10-40 $^{\circ}$C min^{-1}. Active pyrolysis for the decomposition of jeans waste occurred at temperatures ranging from 250 to 550 $^{\circ}$C. Specific Coats-Redfern-type reaction mechanisms were applied to determine the kinetic and thermodynamic variables in the active temperature zone. The thermodynamic parameters (ΔH and ΔG) and activation energies increased when the heating rate was increased from 10 to 30 $^{\circ}$C min^{-1}. When the heating rate was further increased to 40 $^{\circ}$C min^{-1}, ΔH, ΔG, and the activation energies decreased. For heating rates of 10, 20, 30, and 40 $^{\circ}$C min^{-1}, the pre-exponential factors varied in the ranges of 7.4×10^3 to 1.4×10^4, 1.8×10^4 to 5.1×10^{10}, 2.8×10^4 to 5.3×10^{10}, and 3.6×10^4 to 3.1×10^{10} min^{-1}, respectively. In each reaction mechanism model, the entropy changed negatively for all the heating rates examined in this study. This work and its results could serve as a guide for implementing such pyrolysis processes for textile wastes at a practical scale for bioenergy applications.

Keywords: Jeans Waste, Pyrolysis, Thermal Decomposition, Kinetics, Thermodynamics

INTRODUCTION

Modern life is the result of industrialization, which, in turn, is based on utilizing copious amounts of energy in various forms, such as electricity, transportation, heating, and steam [1,2]. Currently, most of the energy supply is based on fossil fuels such as coal, crude oil, and natural gas [3]. To keep pace with global developments, the amount of energy used will continue to increase over time [4,5]. However, the usage of fossil fuels is accompanied by severe issues such as the finite and unequal distribution of reserves, politics, and energy trade policies to meet current energy demands. Arguably, the most significant among these issues are the environmental issues such as global warming and greenhouse gas emissions [2,6]. To continue global national development and maintain a modern lifestyle, it is crucial to find new alternative sources of energy and also establish a sustainable cycle of energy production and trade [1,7].

The issues currently encountered when using fossil fuels have generated global attention toward utilizing renewable and sustainable biomass [8,9]. Recycling and the reusability are the viable options to convert biomass into valuable products such as energy or petroleum [10,11]. Textile waste constitutes a significant proportion of biomass, which can be converted into value-added products and energy [12]. The volume of textile waste produced annually is currently 1.5 billion tons, and it is expected to reach approximately 8.95 billion tons by 2050. This increase would be due to improved living standards and the increased consumption of clothing [13]. Among all the types of textile wastes, denim or jeans waste is considered the most widely and consistently produced waste, because 2.16 million tons of jeans waste is accessible annually [14]. Nearly 75% of the fabric materials that cannot be reprocessed are processed via simple incineration, releasing noxious gases that adversely impact the environment [15].

†To whom correspondence should be addressed.
E-mail: hassanzeb.ieee@pu.edu.pk, jaehoonkim@skku.edu

Textile waste contains a fibrous cellulosic backbone because it is made up of 80-95% of cellulosic material, along with protein, ash, peptic substance, organic acid, wax and sugar attached to different types of hydrogen bonds which makes it complex in nature [16]. Therefore, using thermochemical conversion techniques such as pyrolysis, gasification, and combustion to convert these wastes into energy-dense products and valuable chemicals that can serve as fossil resource substitutes appears feasible [17-19]. The pyrolytic decomposition of jeans waste is potentially the most viable option among all the thermochemical techniques, owing to its high economic feasibility, facile scale-up, and fast reaction [19,20]. Pyrolysis is the thermochemical disintegration of a material at moderate temperatures (250-600 °C) under a non-oxidative environment to produce various types of end products (such as bio-oil, biogas, and bio-char) [21,22]. The efficient operation of pyrolysis depends on various operational parameters, such as the temperature, heating rates, properties of the raw feed, type of pyrolyzer and type of catalysts [23-29].

Despite the significant potential of textile waste, only a few studies have reported on the production of bio-oil, char, and syngas by using pyrolysis under different reaction conditions. Zeng et al. [30] studied the pyrolysis of denim jeans waste to produce activated carbon at low temperatures. Yousef et al. [31] evaluated the possibility of bioenergy production from jeans waste using a small-scale pyrolysis apparatus. Although previous studies have demonstrated the high feasibility of pyrolyzing jeans waste, there still exists a lack of comprehensive studies on the kinetic and thermodynamic analysis of textile wastes during pyrolysis. Such an analysis is a prerequisite for implementation on a practical scale. Therefore, this study aims to provide information regarding the thermal breakdown properties of jeans waste and understand the changes in the kinetic and thermodynamic profiles under different heating rates (10, 20, 30, and 40 °C min^{-1}) by employing the Coats-Redfern method [32]. All the calculations were based on data from a thermogravimetric analyzer, which is an important tool used to observe the conversion behaviors during thermochemical conversion processes [33].

MATERIALS AND METHODOLOGY

1. Sample Preparation and Characterization

A pair of jeans was dried under sunlight to evaporate the surface-absorbed moisture and then dried in an electric oven at 100 °C for 48 h to eliminate the bound moisture. After being dried, the jeans were reduced in size to 0.1-0.5 mm using a shredder connected to a sizer. A proximate analysis, using an electric oven and a muffle furnace, and an ultimate analysis, using CHNS elemental analysis (ThermoScientific, Flash 2000, Austria), were performed to determine the elemental and physicochemical properties of the jeans. A bomb calorimeter (Parr Instrument Company, 6200 Isoperibol Calorimeter) was used to calculate the higher heating value (HHV) of the jeans sample. The chemical functional groups present in the jeans sample were identified by Prestige-19 Fourier transform infrared spectroscopy (FT-IR) (Shimadzu Corporation, Japan). The analysis was performed by casting pellets of the jeans sample with KBr in a ratio of 1 : 100. The IR scanning range was 400-4,000 cm^{-1}, with a resolution of 4 cm^{-1}. The thermal decomposition behavior of the

jeans sample under the pyrolysis conditions was observed using a thermogravimetric analyzer (LECO, USA, TGA 701) in a N$_2$ environment at 25-800 °C. The flow rate of N$_2$ was fixed at 100 mL min^{-1}; however, the heating rate was varied in the 10-40 °C min^{-1} range. During heating, the weight loss and its rate were measured with respect to the temperature and time. Lower heating rates of 10-40 °C min^{-1} were selected to control the heat transfer boundaries. Thermogravimetric analysis (TGAs) was conducted at least thrice and the average values were recorded. The statistics obtained from the TGA profiles allowed us to understand the thermal decomposition behavior during the pyrolysis process. Thus, we could evaluate the kinetics and thermodynamic parameters.

2. Kinetic Analysis

The kinetic parameters for the pyrolysis of the jeans sample were estimated using the Arrhenius law, as shown in Eq. (1), which provided information regarding the reaction rates:

$$\frac{d\alpha}{dt} = k(T)f(\alpha) \tag{1}$$

In Eq. (1), (T), R is the gas constant (0.008314 kJ mole^{-1} K^{-1}), and α is a conversion factor, whose value was determined using Eq. (2):

$$\alpha = \frac{(w_i - w_0)}{(w_i - w_f)}, \tag{2}$$

where w_i and w_f represent the initial and final weights of the samples, respectively, and w_0 represents the weight of the sample at a specific point. By combining and integrating Eqs. (1) and (2), Eq. (3) was derived:

$$\ln\left(\frac{g(\alpha)}{T^2}\right) = \ln\frac{AR}{\beta E_a}\left(1 - \frac{2RT}{E_a}\right) - \frac{E_a}{RT} \tag{3}$$

In Eq. (3), g(α) is an integral function, which varies for different reaction mechanisms, as listed in Table 1, and β is the heating rate. Eq. (3) is known as the equation of the Coats-Redfern model. The Coats-Redfern model is a model-fitting approach that can be used to predict the activation energy (E$_a$) and the pre-exponential factor (A). The values of E$_a$ and A can be obtained by calculating the slope and intercept of the 1/T vs. ln[g(α)/T^2] plot.

3. Thermodynamic Analysis

Thermodynamic parameters were derived from the TGA and kinetic data; these included the change in enthalpy (ΔH) which was calculated using ΔH=E$_a$−RT, and the change in Gibbs free energy (ΔG), which was determined using $\Delta G = E_a + RT_m\ln\left(\frac{K_B T_m}{hA}\right)$, where K$_B$ denotes the Boltzmann constant (1.381×10^{-23} m^2 kg s^{-2}), h represents Planck's constant (6.626×10^{-34} m^2 kg s^{-1}), and T$_m$ is the peak temperature at which maximum weight loss occurs. The change in entropy (ΔS) was calculated using ΔS=ΔH−ΔG/T$_m$.

RESULTS AND DISCUSSION

1. Characterization of Jeans

Results of the proximate and ultimate analysis of the jeans waste are presented in Table 2. The volatile matter content was signifi-

Table 1. Kinetic and conversion functions and the corresponding mechanisms used in the Coats-Redfern method [32,34]
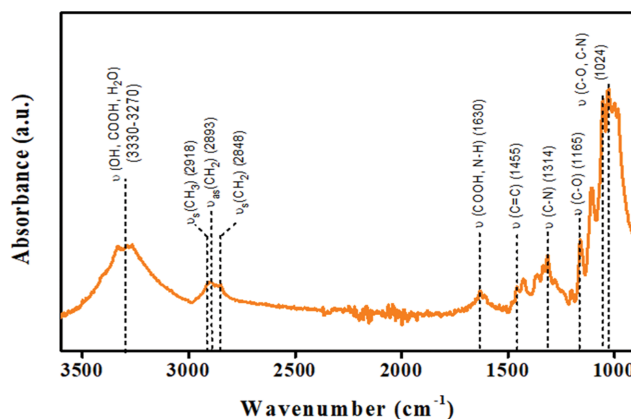
Model name	Mechanism	Symbol	f(α)	g(α)
Reaction order model	Zero-order F0	F0	1	α
	First-order F1	F1	$(1-\alpha)$	$-\ln(1-\alpha)$
	Second-order F2	F2	$(1-\alpha)^2$	$(1-\alpha)^{-1}-1$
	Third-order F3	F3	$(1-\alpha)^3$	$0.5[(1-\alpha)^{-2}-1]$
Diffusivity model	1-D diffusion D1	D1	$\alpha^2/2$	α^2
	2-D diffusion D2	D2	$[-\ln(1-\alpha)]^{-1}$	$[(1-\alpha)\ln(1-\alpha)]+\alpha$
	3-D diffusion-Jander Eq.	D3	$2(1-\alpha)^{2/3}[1-(1-\alpha)^{1/3}]^{-1}$	$[1-(1-\alpha)^{1/3}]^2$
	Ginstling–Brounstein	D4	$(3/2)[(1-\alpha)^{-1/3}-1]^{-1}$	$1-\tfrac{2}{3}\alpha-(1-\alpha)^{2/3}$
Power law	Power law	P2	$2\alpha^{3/4}$	$\alpha^{1/4}$
	Power law	P3	$3\alpha^{2/3}$	$\alpha^{1/3}$
Geometrical contraction models	Contracting cylinder	R2	$2(1-\alpha)^{1/2}$	$1-(1-\alpha)^{1/2}$
	Contracting sphere	R3	$3(1-\alpha)^{2/3}$	$1-(1-\alpha)^{1/3}$
Nucleation models	Avrami-Erofeev	A2	$2(1-\alpha)[-\ln(1-\alpha)]^{1/2}$	$[-\ln(1-\alpha)]^{1/2}$
	Avrami-Erofeev	A3	$3(1-\alpha)[-\ln(1-\alpha)]^{2/3}$	$[-\ln(1-\alpha)]^{1/3}$

Table 2. Proximity and ultimate analysis of the jeans waste sample

Proximate analysis (wt%)	
Moisture	6.8
Volatile matter	90.1
Fixed carbon	2.2
Ash	0.9
Ultimate analysis (wt%)	
C	48.6
H	5.7
S	0.5
N	3.5
O (by difference)	42.0
HHV (MJ kg^{-1})	17.14

Fig. 1. FT-IR spectrum of the jeans waste sample used in this study.

cantly high (90.1%), whereas the fixed carbon and ash content was considerably low, 2.2% and 0.9%, respectively. Furthermore, the carbon and hydrogen content was 48.6 wt% and 5.7 wt%, respectively. The HHV was 17.14 MJ kg^{-1}, which is within the range of the typical calorific value of biomass (15-19 MJ kg^{-1}). Therefore, based on the proximate and ultimate analysis and its calorific value, jeans waste is deemed as a suitable feedstock to produce renewable fuels via thermal conversion techniques [31,35].

The FT-IR spectrum (Fig. 1) of the dried jeans waste exhibited hydroxyl (ν-C-OH at 3,330-3,270 cm^{-1}, including vibration from COOH and adsorbed H$_2$O), carboxyl (ν-COOH at 1,630 cm^{-1}), and ether (ν-C-O at 1,170-1,020 cm^{-1}) groups that corresponded to the oxygenated functionalities associated with cotton. In addition, the jeans sample exhibited symmetric CH$_3$ stretching vibration at 2,918 cm^{-1}, asymmetric CH$_2$ stretching vibration at 2,893 cm^{-1}, and symmetric CH$_2$ stretching vibration at 2,848 cm^{-1} [36]. The presence of a C=C group peak at 1,455 cm^{-1} and a C-N group peak at 1,314 cm^{-1} corresponded to the skeletal vibration of aromatic rings and the vibration of aromatic amines [37], which could be attributed to the indigo dye.

2. Thermogravimetric Analysis

Fig. 2 illustrates the TGA and the differential thermogravimetric analysis (DTA) profiles of the jeans waste under different heating rates in the 10-40 °C min^{-1} range. The TGA profiles can be divided into four regions. The weight loss in the low-temperature region (50-150 °C) was attributed to the evaporation of inbound moisture and low volatile hydrocarbons [38]. The weight loss in the medium-temperature region (200-350 °C) corresponded to the decomposition of thermally labile species such as organic acids and cellulosic material. Similarly, the weight loss in the high-temperature region (400-550 °C) could have originated from the disintegration of protein and fatty acids. The maximum conversion of Jeans waste occurred in the range of 200-550 °C and hence the region is denoted as the active pyrolysis zone [38,39]. Furthermore, the gradual weight loss above 550 °C implied the thermal degradation of mineral salts in the form of metal additives such as Fe, Cu, Al, Zn, Ti, Cr, Ni, etc. [40].

Fig. 2(b) shows the DTA curves at different heating rates ranging from 10 to 40 °C min^{-1}, which provided distinctive pyrolysis temperatures and fractional weight losses. In the active thermal pyro-
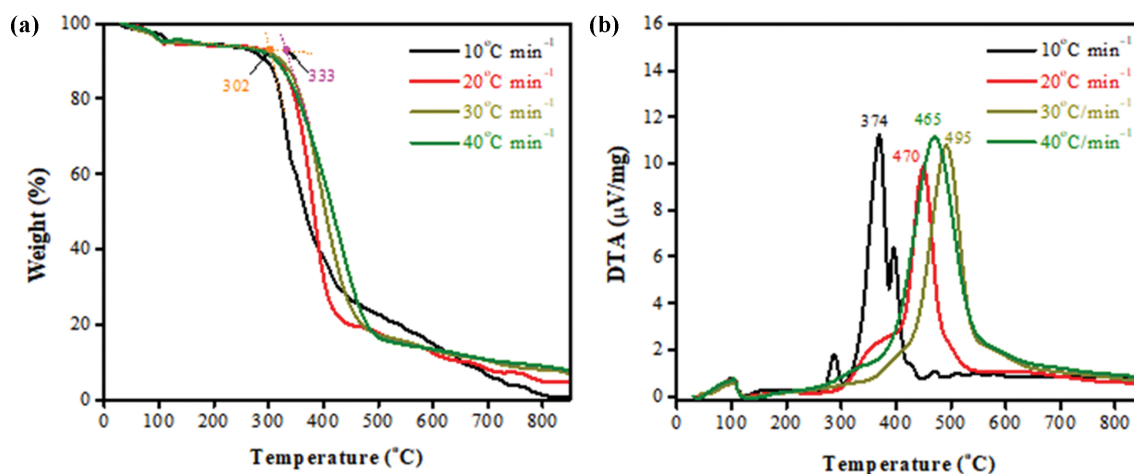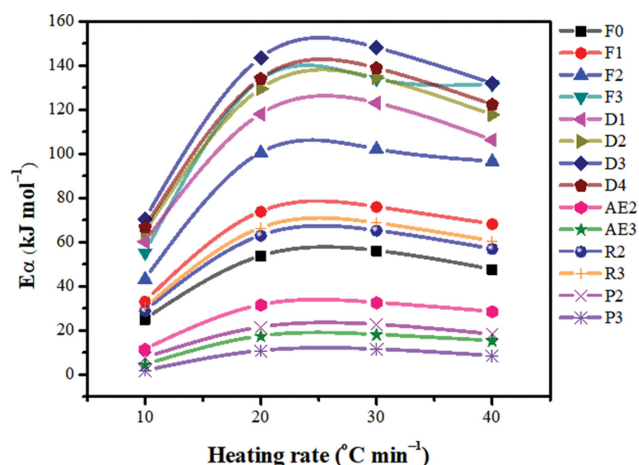
Fig. 3. Activation energy at 10, 20, 30, and 40 °C min⁻¹ obtained using different mechanism models of the Coats-Redfern method.

values of E_a, R^2, and the pre-exponential factor A in the active pyrolysis zones. The kinetic variables were measured at heating rates of 10-40 °C min⁻¹ using the reaction models considered in this study. The linear regression values, R^2, obtained at higher heating rates (30 and 40 °C min⁻¹) were closer to 1 than those obtained at lower heating rates (10 and 20 °C min⁻¹). This was especially true for the nucleation growth (AE2 and AE3), power-law (P2 and P3), and geometric contraction models (R2 and R3).

As shown in Fig. 3, all the chemical reaction models indicate that E_a increases when the heating rate increases to 30 °C min⁻¹, but then decreases when the heating rate is further increased to 40 °C min⁻¹. The three-dimensional diffusion-Jander equation model produced the highest E_a values at all the heating rates examined in this study. However, the power-law P3 model produced the lowest

E_a values among all the reaction models. The value of A increased as the heating rate increased from 10 to 30 °C min⁻¹. It then decreased when the heating rate was further increased to 40 °C min⁻¹. A is associated with the amount of time taken by the molecules to collide at the angles required to proceed with a reaction [47]. A smaller value of A ($\leq 10^9$ s⁻¹) indicates that more surface reactions occurred due to limitations in the rotation of the particles in the activated complex reagent with respect to its initial substance. However, larger values of A ($>10^9$ s⁻¹) indicate that the sample is composed of loosely bound complex molecules [41]. The pre-exponential factors were 7.4×10^3-9.9×10^3, 1.8×10^4-5.1×10^{10}, 2.8×10^4-5.3×10^{10}, and 3.6×10^4-3.1×10^{10} min⁻¹ at heating rates of 10, 20, 30, and 40 °C min⁻¹, respectively. Therefore, the pre-exponential factors increased with the heating rates because of the increased number of collisions between the molecules [43].

4. Thermodynamic Analysis

The thermodynamic variables (ΔH, ΔG, and ΔS) were estimated at heating rates of 10-40 °C min⁻¹ by applying different categories of equations of the reaction mechanism models based on the Coats-Redfern method; the corresponding results are listed in Table 4. The change in ΔH is a state function that provides information regarding the heat absorption and heat release during the reaction [48]. All the reaction mechanism models exhibited positive ΔH values in the active pyrolysis zone under each heating rate. A positive ΔH value indicates that heat from an external resource is required to produce the reagents at higher energy levels in their conversion state. ΔG is a measure of the energy released when an intermediate complex is formed as a result of bond breakage in the reactants [49]. The ΔS values ranged from −0.1756 to −0.1809 (10 °C min⁻¹), −0.0518 to −0.1752 (20 °C min⁻¹), −0.0526 to −0.1707 (30 °C min⁻¹), and −0.0559 to −0.1694 kJ mol⁻¹ (40 °C min⁻¹). The negative ΔS values indicate decreased randomness in the products, as

Table 4. Thermodynamic parameters of jeans waste at 10, 20, 30, and 40 °C min⁻¹ obtained using the Coats-Redfern method

|	Temperature (200-500 °C)											
	10			20			30			40		
Model	(°C min⁻¹)											
	ΔH	ΔG	ΔS	ΔH	ΔG	ΔS	ΔH	ΔG	ΔS	ΔH	ΔG	ΔS
	(kJ mol⁻¹)											
F0	21.93	89.61	−0.1809	49.71	131.63	−0.1743	51.99	136.33	−0.1707	43.72	122.42	−0.1692
F1	29.96	97.62	−0.1809	69.88	143.15	−0.1559	71.83	146.95	−0.1520	64.28	138.99	−0.1606
F2	40.07	107.61	−0.1805	96.60	147.99	−0.1093	98.00	150.97	−0.1072	92.63	146.23	−0.1152
F3	52.08	117.77	−0.1756	129.54	153.91	−0.0518	129.79	155.81	−0.0526	127.65	153.67	−0.0559
D1	57.06	124.09	−0.1792	114.13	159.62	−0.0967	118.98	163.30	−0.0897	102.47	156.33	−0.1158
D2	61.76	128.62	−0.1787	125.58	164.31	−0.0824	130.28	167.79	−0.0759	113.84	161.29	−0.1020
D3	67.30	134.10	−0.1786	139.60	172.70	−0.0704	144.05	176.08	−0.0648	128.18	170.11	−0.0901
D4	63.57	130.87	−0.1799	130.15	171.02	−0.0869	134.77	174.67	−0.0807	118.50	168.09	−0.1066
AE2	8.38	76.06	−0.1809	27.58	109.91	−0.1751	28.41	113.28	−0.1718	24.63	103.40	−0.1694
AE3	1.19	68.87	−0.1809	13.46	95.798	−0.1751	13.91	98.79	−0.1718	11.38	90.169	−0.1694
R2	25.69	93.36	−0.1809	58.99	139.93	−0.1722	61.13	144.35	−0.1684	53.05	131.51	−0.1687
R3	27.06	94.73	−0.1809	62.44	142.92	−0.1712	64.52	147.17	−0.1673	56.58	134.92	−0.1684
P2	4.37	72.05	−0.1809	17.50	99.83	−0.1752	18.49	103.37	−0.1718	14.35	93.135	−0.1694
P3	1.48	66.18	−0.1809	6.74	89.08	−0.1751	7.31	92.18	−0.1718	4.54	83.32	−0.1694
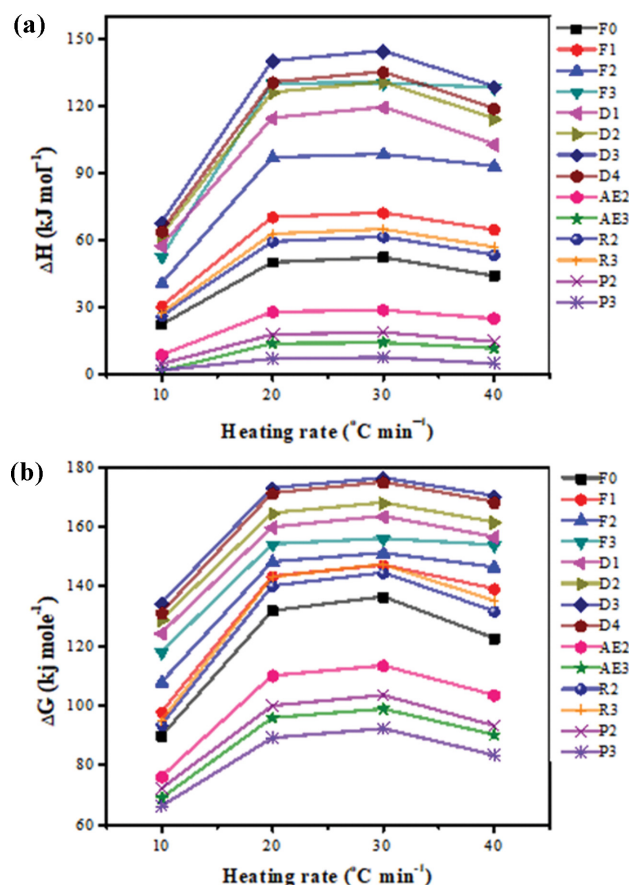
Fig. 4. Values of (a) ΔH and (b) ΔG at heating rates of 10, 20, 30, and 40 °C min⁻¹, estimated using the different mechanism models of the Coats-Redfern method.

compared to the raw jeans waste. Thus, it was inferred that the thermal decomposition of jeans waste is not a spontaneous reaction [24,50].

Figs. 4(a) and (b) show that ΔH and ΔG increase as the heating rate increases from 10 to 30 °C min⁻¹; however, these values decrease when the heating rate further increases to 40 °C min⁻¹ in all the reaction mechanism models of the Coats-Redfern method. This is because the calculation of ΔH and ΔG depends on the TGA data and kinetic parameters and, thus, the trends are identical to those of the previous kinetic parameters. The 3-D diffusion-Jander equation model produced the highest ΔH and ΔG values at all the heating rates. However, the power-law P3 model produced the lowest ΔH and ΔG values among all the reaction models.

CONCLUSIONS

This study analytically inspected the thermal decomposition and kinetic and thermodynamic parametric profiles of a jeans waste sample which contained a complex composition of 80-95% cellulosic material along with protein, peptic material, organic acid, sugar and wax. The TGA and DTG data indicated that jeans waste pyrolysis is an intricate process involving multiple reactions. The effect of varying heating rates with weight loss and the thermo-kinetic profiles was evaluated. Thermo-kinetic calculations were performed

using the Coats-Redfern method in the active pyrolytic zone (200-550 °C). In each model, E_a, ΔH, and ΔG increased when the heating rate increased from 10 to 30 °C min⁻¹, at which the maximum values were obtained. These parameters subsequently began to decrease upon a further increment in the heating rate to 40 °C min⁻¹. Higher heating rates provided an improved correlation coefficient R^2 than the lower heating rates. The kinetic and thermodynamic parameters enabled us to understand the reaction mechanism, conversion rate, and energy profile. This could, in turn, provide valuable information pertaining to the implementation of the pyrolysis process on a practical scale for bioenergy applications.

REFERENCES

1. F. A. Brones, M. M. Carvalho and E. S. Zancul, *J. Clean. Prod.*, **142**, 8 (2017).
2. H. Rezk, A. M. Nassef, A. Inayat, E. T. Sayed, M. Shahbaz and A. G. Olabi, *Sci. Total Environ.*, **658**, 1150 (2019).
3. S. A. Sarkodie and V. Strezov, *Sci. Total Environ.*, **639**, 888 (2018).
4. M. Nazar, A. Yasar, S. A. Raza, A. Ahmad, R. Rasheed, M. Shahbaz and A. B. Tabinda, *Biomass Convers. Biorefin.*, **11**, 1 (2021).
5. J.-M. Ha, K.-R. Hwang, Y.-M. Kim, J. Jae, K. H. Kim, H. W. Lee, J.-Y. Kim and Y.-K. Park, *Renew. Sust. Energ. Rev.*, **111**, 422 (2019).
6. S. Oh, J. Lee, S. S. Lam, E. E. Kwon, J.-M. Ha, D. C. W. Tsang, Y. S. Ok, W.-H. Chen and Y.-K. Park, *Bioresour. Technol.*, **342**, 126067 (2021).
7. M. Shahbaz, A. AlNouss, P. Parthasarathy, A. H. Abdelaal, H. Mackey, G. McKay and T. Al-Ansari, *Biomass Convers. Biorefin.*, **12**, 669 (2020).
8. S. Polat and P. Sayan, *Energ. Source. Part A.*, **42**, 1 (2020).
9. J.-Y. Kim, H. W. Lee, S. M. Lee, J. Jae and Y.-K. Park, *Bioresour. Technol.*, **279**, 373 (2019).
10. J. Lee, E. E. Kwon, S. S. Lam, W.-H. Chen, J. Rinklebe and Y.-K. Park, *J. Clean. Prod.*, **321**, 128989 (2021).
11. C. Park and J. Lee, *Int. J. Energy Res.*, **45**, 13088 (2021).
12. L. J. R. Nunes, R. Godina, J. C. O. Matias and J. P. S. Catalão, *J. Clean. Prod.*, **171**, 1353 (2018).
13. M. del Mar Barbero-Barrera, O. Pombo and M. de los Angeles Navacerrada, *Compos. B. Eng.*, **94**, 26 (2016).
14. R. Paul, *Denim*, Woodhead Publishing, United Kingdom (2015).
15. X. Meng, W. Fan, Y. Ma, T. Wei, H. Dou, X. Yang, H. Tian, Y. Yu, T. Zhang and L. Gao, *Text. Res. J.*, **90**, 695 (2020).
16. P. Peña-Pichardo, G. Martínez-Barrera, M. Martínez-López, F. Ureña-Núñez and J. M. L. dos Reis, *Constr. Build. Mater.*, **177**, 409 (2018).
17. H. Dahlbo, K. Aalto, H. Eskelinen and H. Salmenperä, *Sustain. Prod.*

Consum., **9**, 44 (2017).

18. C. Wen, Y. Wu, X. Chen, G. Jiang and D. Liu, *J. Therm. Anal. Calorim.*, **128**, 581 (2017).

19. A. Hanoğlu, A. Çay and J. Yanık, *Energy J.*, **166**, 664 (2019).

20. X. Chen, Y. Chen, H. Yang, W. Chen, X. Wang and H. Chen, *Bioresour. Technol.*, **233**, 15 (2017).

21. M. W. Seo, S. H. Lee, H. Nam, D. Lee, D. Tokmurzin, S. Wang and Y.-K. Park, *Bioresour. Technol.*, **343**, 126109 (2022).

22. S. Jung, N. P. Shetti, K. R. Reddy, M. N. Nadagouda, Y.-K. Park, T. M. Aminabhavi and E. E. Kwon, *Energy Convers. Manag.*, **236**, 114038 (2021).

23. Q. T. Trinh, A. Banerjee, K. B. Ansari, D. Q. Dao, A. Drif, N. T. Binh, D. T. Tung, P. M. Q. Binh, P. N. Amaniampong and P. T. Huyen, *Biorefinery of alternative resources: Targeting green fuels and platform chemicals*, Springer, Singapore (2020).

24. S. R. Naqvi, R. Tariq, Z. Hameed, I. Ali, S. A. Taqvi, M. Naqvi, M. B. K. Niazi, T. Noor and W. Farooq, *Fuel*, **233**, 529 (2018).

25. S. Yousef, M. Tatariants, M. Tichonovas, Z. Sarwar, I. Jonuškienė and L. Kliucininkas, *Resour. Conserv. Recycl.*, **145**, 359 (2019).

26. J. Lee, E. E. Kwon and Y.-K. Park, *Catal. Today*, **355**, 263 (2020).

27. Y.-M. Kim, J. Jae, B.-S. Kim, Y. Hong, S.-C. Jung and Y.-K. Park, *Energy Convers. Manag.*, **149**, 966 (2017).

28. S. Valizadeh, S. S. Lam, C. H. Ko, S. H. Lee, A. Farooq, Y. J. Yu, J.-K. Jeon, S.-C. Jung, G. H. Rhee and Y.-K. Park, *Bioresour. Technol.*, **320**, 124313 (2021).

29. S. Valizadeh, S.-H. Jang, G. Hoon Rhee, J. Lee, P. Loke Show, M. Ali Khan, B.-H. Jeon, K.-Y. Andrew Lin, C. Hyun Ko, W.-H. Chen and Y.-K. Park, *Chem. Eng. J.*, **433**, 133793 (2022).

30. D. Zeng, S. Wang, J. Peng, Y. Gui, H. Liu, F. Yang and M. Li, *ChemistrySelect*, **4**, 7649 (2019).

31. S. Yousef, J. Eimontas, N. Striūgas, M. Tatariants, M. A. Abdelnaby, S. Tuckute and L. Kliucininkas, *Energy Convers. Manag.*, **196**, 688 (2019).

32. S. R. Naqvi, R. Tariq, Z. Hameed, I. Ali, M. Naqvi, W.-H. Chen, S. Ceylan, H. Rashid, J. Ahmad and S. A. Taqvi, *Renew. Energy*, **131**, 854 (2019).

33. G. Mishra, J. Kumar and T. Bhaskar, *Bioresour. Technol.*, **182**, 282

(2015).

34. S. R. Naqvi, Z. Hameed, R. Tariq, S. A. Taqvi, I. Ali, M. B. K. Niazi, T. Noor, A. Hussain, N. Iqbal and M. Shahbaz, *J. Waste Manag.*, **85**, 131 (2019).

35. K. A. Motghare, A. P. Rathod, K. L. Wasewar and N. K. Labhsetwar, *J. Waste Manag.*, **47**, 40 (2016).

36. D. Yoon, K. Y. Chung, W. Chang, S. M. Kim, M. J. Lee, Z. Lee and J. Kim, *Chem. Mater.*, **27**, 266 (2015).

37. T. Szabó, O. Berkesi, P. Forgó, K. Josepovits, Y. Sanakis, D. Petridis and I. Dékány, *Chem. Mater.*, **18**, 2740 (2006).

38. A. Islam, Y. Molla, T. K. Dey, M. Jamal, R. Rathanasamy and M. Uddin, *J. Polym. Res.*, **28**, 1 (2021).

39. D. Zhao, K. Chen, F. Yang, G. Feng, Y. Sun and Y. Dai, *Cellulose*, **20**, 3205 (2013).

40. S. Yousef, M. Tatariants, M. Tichonovas, L. Kliucininkas, S.-I. Lukošiūtė and L. Yan, *J. Clean. Prod.*, **254**, 120078 (2020).

41. Z. Akyürek, *Sustainability*, **11**, 2280 (2019).

42. A. Skreiberg, Ø. Skreiberg, J. Sandquist and L. Sørum, *Fuel*, **90**, 2182 (2011).

43. X. Yang, Y. Zhao, R. Li, Y. Wu and M. Yang, *Thermochim. Acta*, **665**, 20 (2018).

44. W.-H. Chen, C. F. Eng, Y.-Y. Lin and Q.-V. Bach, *Energy Convers. Manag.*, **221**, 113165 (2020).

45. A. Zaker, Z. Chen, M. Zaheer-Uddin and J. Guo, *J. Environ. Chem. Eng.*, **9**, 104554 (2021).

46. G. Xia, W. Han, Z. Xu, J. Zhang, F. Kong, J. Zhang, X. Zhang and F. Jia, *J. Environ. Chem. Eng.*, **9**, 106182 (2021).

47. V. Balasundram, N. Ibrahim, R. M. Kasmani, M. K. A. Hamid, R. Isha, H. Hasbullah and R. R. Ali, *J. Clean. Prod.*, **167**, 218 (2017).

48. X. Yuan, T. He, H. Cao and Q. Yuan, *Renew. Energy*, **107**, 489 (2017).

49. S. C. Turmanova, S. D. Genieva, A. S. Dimitrova and L. T. Vlaev, *Express Polym. Lett.*, **2**, 133 (2008).

50. A. C. M. Loy, D. K. W. Gan, S. Yusup, B. L. F. Chin, M. K. Lam, M. Shahbaz, P. Unrean, M. N. Acda and E. Rianawati, *Bioresour. Technol.*, **261**, 213 (2018).